SCIENTIFIC REPORTS

OPEN

SUBJECT AREAS:
METAMATERIALS
TERAHERTZ OPTICS
OPTICAL PROPERTIES AND DEVICES
PHOTONIC DEVICES

Received
12 February 2013

Accepted
13 June 2013

Published
4 July 2013

Correspondence and requests for materials should be addressed to H.C. (hychoi@yonsei.ac.kr) or B.M. (bmin@kaist.ac.kr)

* These authors contributed equally to this work.

Ultrafast refractive index control of a terahertz graphene metamaterial

Seung Hoon Lee[1]*, Jeongmook Choi[2]*, Hyeon-Don Kim[1], Hyunyong Choi[2] & Bumki Min[1]

[1]Department of Mechanical Engineering, Korea Advanced Institute of Science and Technology (KAIST), Daejeon 305-751, Republic of Korea, [2]School of Electrical and Electronic Engineering, Yonsei University, Seoul 120-749, Republic of Korea.

Modulation of the refractive index of materials is elementary, yet it is crucial for the manipulation of electromagnetic waves. Relying on the inherent properties of natural materials, it has been a long-standing challenge in device engineering to increase the index-modulation contrast. Here, we demonstrate a significant amount of ultrafast index modulation by optically exciting non-equilibrium Dirac fermions in the graphene layer integrated onto a high-index metamaterial. Furthermore, an extremely-large electrical modulation of refractive index up to $\Delta n \sim -3.4$ (at 0.69 THz) is achieved by electrical tuning of the density of the equilibrium Dirac fermion in the graphene metamaterial. This manifestation, otherwise remaining elusive in conventional semiconductor devices, fully exploits the characteristic ultrafast charge relaxation in graphene as well as the strong capacitive response of the metamaterial, both of which enable us to drastically increase the light-matter interaction of graphene and the corresponding index contrast in the graphene metamaterials.

The control of refractive index in natural materials has attracted considerable attention in the field of holographic imaging systems, data storage, and for numerous photonic applications[1]. Changes of refractive index under external stimuli have been studied intensively in various transparent nonlinear crystals[2,3] and light-sensitive materials[4]. However, these natural materials inherently have small index changes due to high-order nonlinearities known as Pockels or Kerr effects, or insignificant modification of molecular structures in polymers. More importantly, fast refractive index modulation in polymer-based materials also is limited significantly by the slow recovery time to the initial state. Therefore, promising alternatives to natural materials for ultrafast index modulation with large contrast are highly desirable. The emergence of artificially-engineered materials, referred to as metamaterials[5,6], enables the manipulation of the electromagnetic properties of materials far beyond the limits of natural materials. By periodically arranging subwavelength-scale metallic elements, both negative and positive indices of refraction were demonstrated recently with extremely high values[7,8]. More interestingly, the tuning ability in the electromagnetic responses in metamaterials, implanted by hybridization with various active media, recently has broadened the field of metamaterial applications[9–15].

Graphene, two-dimensionally arranged carbon atoms in honeycomb lattices, has unique optical absorption properties due to its linear dispersion and the massless nature of its carriers[16]. For example, a monolayer of graphene absorbs ~2.3% of near infrared and visible light due to the universal optical conductivity of the massless Dirac fermion in graphene[17]. This constant and broadband optical absorption shows no Fermi level dependency except near the frequency threshold[18] for interband transitions $\sim 2|E_F|$. However, in the THz regime, where the optical conductivity of graphene is determined mainly by the intraband transitions[19], the optical absorption spectra strongly depend on the Fermi level owing to its band structure. For this reason, the modulation of THz waves using a graphene layer recently was demonstrated successfully by electrically or optically controlling its Fermi level[19–21]. An atomically-thin graphene layer also has a well-known photoconductive nature[22] that can be explained by the diffusion of photo-excited hot carriers with a quasi-Fermi level[23]. The excited carriers undergo a relaxation process that is, in principle, ultrafast (~10 ps at room temperature) owing to the emission of hot optical phonons (phonon energy of $\omega_0 = 196$ meV), in which the energy loss is about an order of magnitude faster than that in conventional semiconductors, such as silicon ($\omega_0 = 63$ meV), germanium ($\omega_0 = 37$ meV), and gallium arsenide ($\omega_0 = 36$ meV)[24–27]. In addition to the ultrafast carrier dynamics of graphene, broadband operation is possible, because the real part of the optical conductivity has nearly non-dispersive values in the THz frequency range[19]. With this end in mind, we concluded that a graphene layer is a promising active medium when integrated with a metamaterial for ultrafast manipulation of broadband THz waves by electrically or optically tuning its refractive index.

Results

Design of graphene metamaterials. To achieve active control of the refractive index in a THz metamaterial, an array of meta-atoms, an atomically thin graphene layer, and an array of metallic wire gate electrodes are functionally configured together into an ultra-compact, thin, and flexible polymeric substrate. The structure of the integrated THz graphene metamaterial designed for large index modulation is shown in Fig. 1a. As an atomically-thin active medium, a monolayer graphene layer was directly deposited onto an array of hexagonal metallic meta-atoms specially designed to have a high index of refraction in the THz frequency range[7]. As can be confirmed by the image of the saturated electric field in Fig. 1c, large numbers of surface charges accumulate on the edge of the hexagonal metallic frame, which induces a significantly large polarization by strong capacitive coupling between the unit cells. Among the accumulated charges, some portion of the charge carriers leak into the attached graphene layer, resulting in a reduction of the induced polarization, which determines the initial refractive index of the graphene metamaterial at the charge neutral point (CNP). When the Fermi level of graphene is tuned by proper electrical gating, the induced polarization is altered because the intraband optical conductivity of graphene is highly sensitive to its Fermi level, and the conductivity change modifies the capacitance between the meta-atoms. With this principle of polarization change, the effective permittivity, and thus the refractive index of the graphene metamaterial can be electrically modulated by applying DC gate voltages. For the electrical tuning of the Fermi level of the graphene layer, a previously reported metallic wire array was used as a gate electrode[15], which was devised to be transparent for the THz waves polarized normal to the wire direction. The transparent gate electrode also is beneficial because it has the possibility of applying a quasi-uniform DC electric field onto the graphene layer, in the same way as is traditionally done with thick and lossy silicon back-gates. An image of the fully-integrated device is shown in Figs. 1b and d, and the geometrical parameters of the fabricated metamaterial are given in the caption of Fig. 1.

Electrical modulation of refractive indices. Figures 2a and b show gate-controlled refractive index Re(n) and figure of merit FOM = Re(n)/Im(n) extracted from the THz-TDS measurement with an iterative algorithm considering multi-pass transmission[7]. At the CNP, a strong electrical resonance was observed with a peak refractive index of 13.8 at a frequency of 0.58 THz and a refractive index of 12.1 at the quasi-static limit where the loss of the metamaterial is minimal. We estimated the charge neutral gate voltage V_{CNP} of the device to be ~120 V from the measured trace of the transmitted THz field maxima (dashed line in Fig. 2). With increasing $|\Delta V|$, where $\Delta V = V_g - V_{CNP}$ and V_g is the applied gate voltage, the LC resonance along with the peak refractive index were red-shifted and the resonance dip was diminished. The phenomenological resonance features of the graphene metamaterial arise from an increase in the real part of the optical conductivity in graphene. At a fixed frequency of 0.69 THz, the refractive index gradually decreased from 12.4 to 9.0 with increasing $|\Delta V|$ due to a remarkable change of the capacitance between the meta-atoms. This unprecedented index contrast ΔRe(n) ~ −3.4 of the graphene metamaterial is much larger than that of any other natural material and hardly obtainable in nature. By conducting numerical simulation using the finite element method

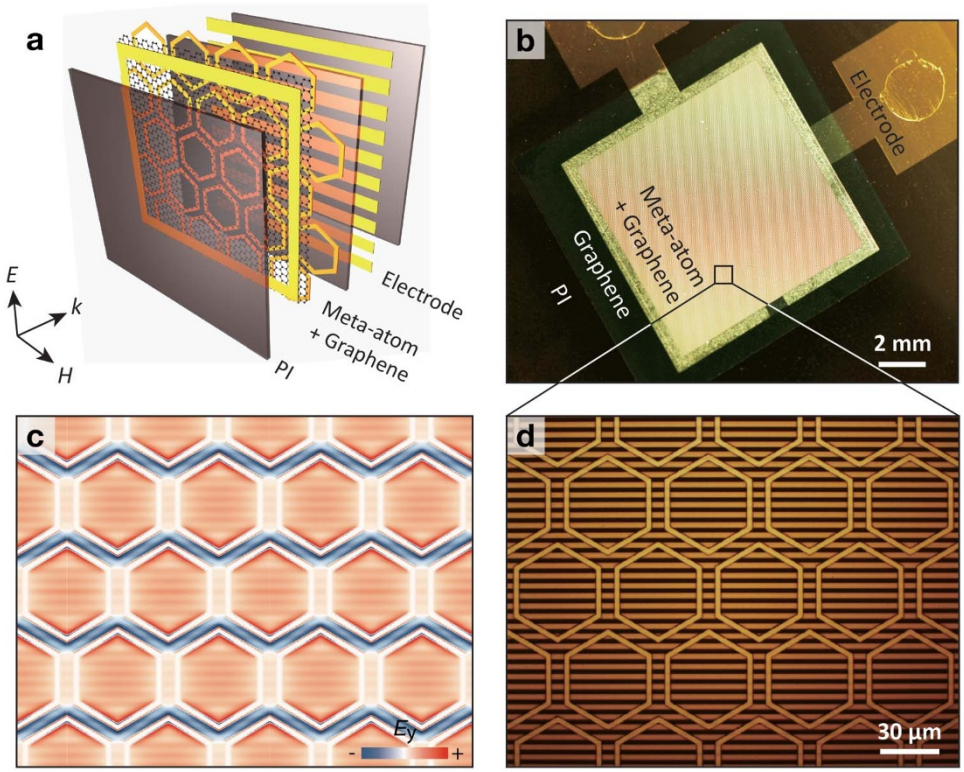

Figure 1 | Schematic view and optical micrograph image of high-index graphene metamaterials. (a) Schematic rendering of a graphene metamaterial shows that a monolayer graphene attached directly to hexagonal gold meta-atoms (a 60-μm-size unit cell with a 3-μm-wide, 100-nm-thick gold frame with a 5-μm-wide gap between adjacent meta-atoms) and transparent wire electrodes (periodicity = 6 μm, metal width = 4 μm) are fully embedded in a thin and flexible polyimide (PI) substrate. The total thickness of the graphene metamaterial was ~3.2 μm, which shows a high index of refraction (above 10) in the THz range. Both the ultrafast optical pump beam and electrical gating contributed to the modulation of the high index of refraction with large index contrast. (b) Optical image of the fabricated high-index graphene metamaterial. (c) In-plane electric field component (at 0.5 THz) of the graphene metamaterial at the CNP. (d) Optical micrograph of the fabricated metamaterial for a clear understanding of the realistic structure of the field image of (c).

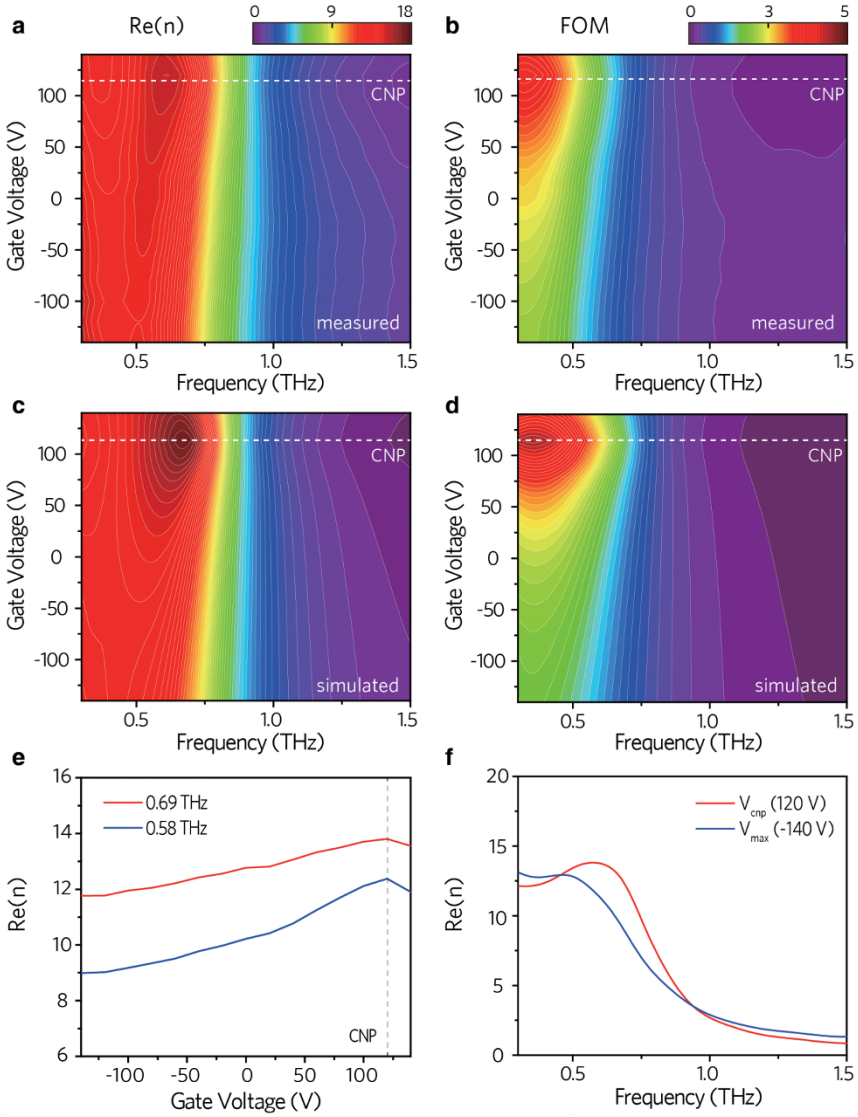

Figure 2 | Electrical control of the refractive index and FOM of the graphene metamaterial. (a) Measured refractive index and (b) figure-of-merit (FOM = Re(n)/Im(n)) plotted as a function of gate voltage. With increased quasi-static carrier density, the refractive index decreases near the resonance frequency. (c) (d) Simulated results with a single-layer graphene approximation corresponding to a and b. Here, we approximated the carrier density at the conductivity minimum and intraband scattering time as 8×10^{11} cm^{-2} and 16 fs, respectively. (e) Gate-dependent refractive indices are presented at frequencies of 0.69 THz and 0.58 THz. At these two frequencies, a maximum index of 14.3 and a maximum index contrast of ~ -3.4 are clearly shown. (f) Frequency-dependent refractive index profile with respect to the two different gate voltages, V_{cnp} and V_{max}. The numbers in parentheses indicate the values of gate voltage.

(FEM), the refractive index and FOM of the proposed metamaterial were reproduced and matched well with the experimental results, as shown in Figs. 2c and d. Considering carrier density at the conductivity minimum[15,28] in CVD-grown graphene to be $n_{min} = 8 \times 10^{11}$ cm^{-2}, the measured refractive index was in excellent agreement with the simulated values over the broadband frequencies.

Optical modulation of refractive indices. To investigate optically-controlled ultrafast index modulation in the graphene metamaterial, we used ultrafast optical-pump THz-probe spectroscopy (See Methods and Supplementary Information). As described in the previous paragraph, the capability of Fermi-level tuning by electrical gating is quite unique, because it enables us to perform ultrafast time-resolved index modulation under various quasi-static operating conditions. As shown in Fig. 3, we measured the pump-induced THz electric field changes $\Delta E(t)$ for each fixed pump-probe delay Δt along with optically unexcited THz field $E_0(t)$. Fourier transform of the measured fields has the information on both real and imaginary values of the pump-induced $\Delta\varepsilon(\omega)$ or $\Delta\sigma(\omega)$. Here, $\Delta\varepsilon(\omega)$ or $\Delta\sigma(\omega)$ denotes the change of dielectric constant or conductivity in the active layer, i.e., meta-atom/graphene layer (For the meta-atom-free samples shown in the Supplementary Information, the values are the change for the graphene layer). As displayed in Fig. 3a, the pump-induced $\Delta E(t)$ traces showed substantial field reshaping compared to the $E_0(t)$. First, we observed negligible phase shifts of $\Delta E(t)$ in the low-frequency part of the early THz field delay ($t < 0$), and apparent phase shifts in the high-frequency component of the THz field ($t > 0$). Second, the opposite sign of $\Delta E(t)$ is significant when $t > 0$, but it is scarcely appreciable when $t < 0$. As discussed later in more detail, these examinations indicate a strong in-phase resonant response at low THz frequencies and an inductive Drude-like behaviour in the high THz frequency range.

The resonant in-phase response was characterized further to corroborate the electrical index modulation in the previous section. As shown in Fig. 3b, when the pump fluence was 18.7 μJ/cm^2, for

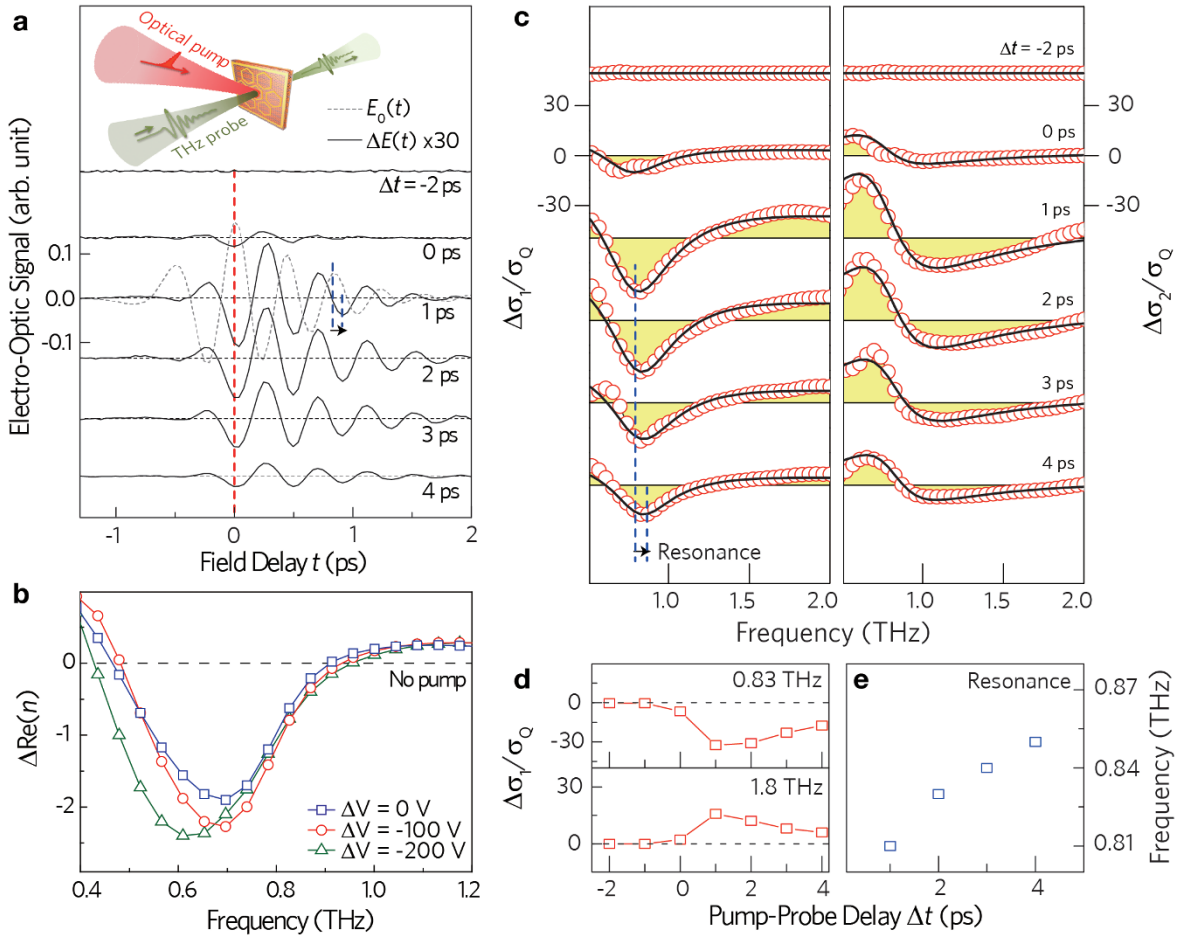

Figure 3 | Ultrafast optical modulation of the refractive index in the graphene metamaterial. (a) Schematic of optical-pump THz-probe spectroscopy. The THz field through the graphene metamaterial without a pump $E_0(t)$ (gray dot) and with a pump (black line) are shown at different pump-probe delays Δt. (b) Gate-dependent refractive index changes at $\Delta t = 1$ ps. The large index contrast $\Delta\mathrm{Re}(n) \simeq -2.4$ and the red-shift of the resonance are clearly visible. (c) Photo-excited conductivity changes (red circle) in the active graphene layer of the metamaterial at a pump fluence of 18.7 μJ/cm^2 near the CNP. The graphene layer shows a negative sign of the differential conductivity change near the resonance frequency. (d) Conductivity changes at 0.83 THz and 1.8 THz show opposite sign. (e) Resonance frequency (parameters from Drude-Lorentz model) was slightly blue-shifted from $\Delta t = 1$ to 4 ps due to the decrease of the graphene's intraband optical conductivity.

example, the photo-induced change in the refractive index showed a large index contrast $\Delta\mathrm{Re}(n) \simeq -2.4$ at around 0.61 THz, and the modulation depth was highly sensitive to the gate voltages that were applied. We note that this large negative-index modulation is hardly observable in any natural photorefractive materials or nonlinear crystals. In addition, the red-shift of peak refractive index with an applied gate voltage was clearly resolved as the gated Fermi level was gradually detuned from the CNP. This behaviour is due to the increased THz conductivity, and it is consistent with the previously described electrical index modulation.

To substantiate our observations, we present the transient dynamics of $\Delta\sigma(\omega)$ for each pump delay Δt at the CNP in Fig. 3c. Immediately after photo-excitation, the real part of conductivity $\Delta\sigma_1(\omega)$ exhibited an asymmetric frequency-dependent reduction $\Delta\sigma_1(\omega) < 0$ near resonance frequency. Likewise, the imaginary part $\Delta\sigma_2(\omega)$ showed complementary zero-crossing, exactly at the resonance frequency. The signs and shapes of these conductivity spectra indicate an increased on-resonance transmission due to the increase of leakage current into the graphene layer and the corresponding reduction of the capacitive coupling between the meta-atoms (Fig. 3d). These features were further confirmed by examining the time-dependent shifts of the resonance frequency as a function of pump-probe delays (Fig. 3e). During the carrier relaxation process ($\Delta t = 1 \sim 4$ ps), the resonance was slightly shifted to higher frequency because the carrier recombination process induces $\Delta\sigma_1(\omega)$ to decrease, and consequently leads to an increased capacitive-coupling between the adjacent meta-atoms. This behaviour agrees qualitatively with the time-domain in-phase analysis described above as well as with the electrically-controlled index changes in the previous section. In addition, this distinct resonant behaviour was ensured by performing the same experiment and checking $\Delta\sigma(\omega)$ on the same sample without the metamaterial as a control sample (See Supplementary Information for the change in the non-equilibrium conductivity of the control sample). As expected, no strong resonance was observed over the entire frequency range; the measured spectra were featureless with broadened $\Delta\sigma_1(\omega)$ by the grain-boundary-limited charge back-scattering in the Drude response[29].

Ultrafast carrier dynamics of graphene metamaterials. To understand the nature of ultrafast index modulation, we investigated the gate-dependent non-equilibrium THz dynamics. Figure 4a is a plot of the negative transmission change $-\Delta T(t)/T = -[2\Delta E(t)/E_0 + (\Delta E(t)/E_0)^2]$ at a fixed field delay at $t = 0$ as a function of the applied gate-voltage. As discussed above, the in-phase response (no phase shift) at early field delay justifies that the overall dynamics is determined by measuring the changes in peak $\Delta E(t)$. The maximum $\Delta E(t)$ occured within the time-resolution of our THz pulse (~1 ps), and the relaxation signal contained multi-exponential

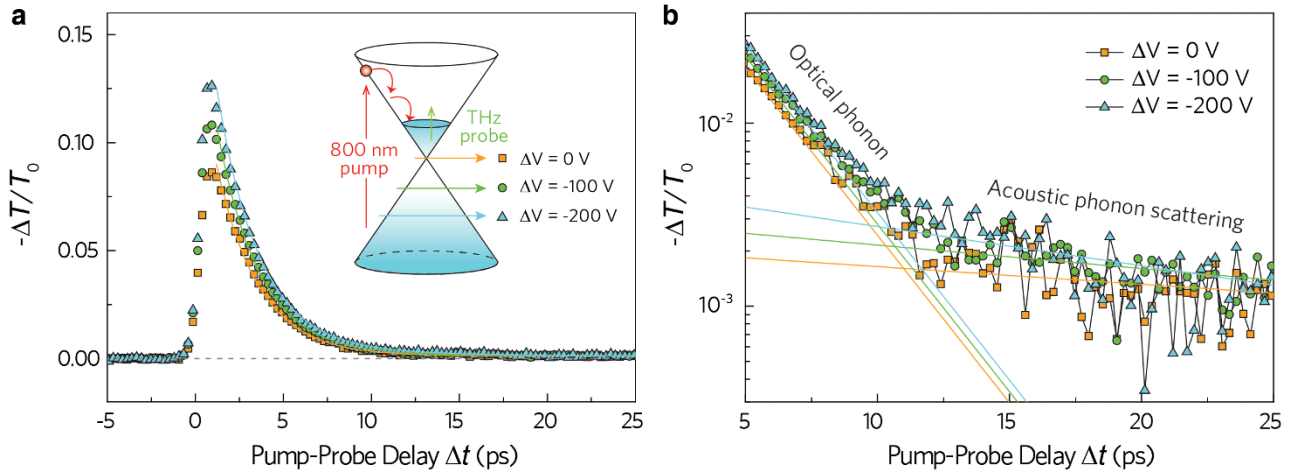

Figure 4 | Ultrafast dynamics of photoexcited carriers in the graphene metamaterial. (a) Negative transmission change ($-\Delta T/T_0$) at 18.7 μJ/cm^2 pump fluence at three different gate voltages ($\Delta V = 0$ V, -100 V, -200 V). The measured values are fitted by a solid line using a bi-exponential decay function. Inset: The band diagram of a monolayer graphene with gate-dependent Fermi levels. (b) Enlarged view of (a) with a logarithmic scale of the transmission. The two fitting lines at each gate voltage intersected at different pump-probe delays. We attributed the slow decay to the acoustic phonon scattering. Early emergence of the slow decay with increasing gate voltage is clearly shown.

decaying components. Note that the data showed a strong gate-dependent feature for the peak $\Delta E(t)$ changes. In contrast to the interband optical spectroscopy, where the transmission changes of the optical probe pulse (typically $>2|E_F|$) are dominated largely by the photo-excited carrier density, the THz spectroscopy is highly sensitive to the initial Fermi level of graphene, since it read the carrier distribution in all energy spectra, including the initial carrier density as well as the photo-excited carrier density. As shown in Fig. 4b, more detailed analysis exhibited that a bi-exponential fit using $(1 - B)\exp(-t/\tau_1) + (B)\exp(-t/\tau_2)$ properly described the THz transient dynamics; we found that a mono-exponential fit did not reproduce the data. Using a logarithmic scale, the data seemingly represented two different time scales. We attributed the picosecond fast relaxation component τ_1 to the optical phonon emission ($\omega_0 = 196$ meV) of the excited hot Dirac fermions and the other τ_2 to the slow acoustic phonon scattering of low-energy carriers[23,26,27,30]. Combining the two relaxation components with the gate-dependent dynamics, we observed that both the amplitude B and the corresponding scattering rate $1/\tau_2$ of the slow relaxation rate became larger with increasing $|\Delta V|$. This implied that the effect of acoustic phonon scattering emerged earlier under high carrier density[26,31]. Given the photo-excited carrier density ($\simeq 1.2 \times 10^{12}$ cm^{-2}), it is well known that the initially photo-excited hot Dirac fermions share their energy with the existing cold carriers (densities determined by $|\Delta V|$) through an ultrafast thermalisation process. As $|\Delta V|$ increased, the initial carrier temperature after thermalisation decreased so that the excited carriers had less chance to emit multiple optical phonons[26], thereby exhibiting the observed early emergence of acoustic phonon cooling as the dominant relaxation mechanism. Thus, the ultimate speed of ultrafast index modulation was limited largely by these persistent cooling dynamics of hot Dirac fermions.

Discussion

By the electrical and/or optical tuning of the Fermi level of monolayer graphene, capacitive coupling between unit cells of graphene-attached metamaterial can be controlled, causing a corresponding change of the effective index of refraction. Based on this principle, we designed high-index THz metamaterials integrated with a CVD-grown monolayer graphene, and transparent electrodes embedded in an optically thin ($\sim\lambda/150$) flexible polyimide substrate. First, electrical modulation showed that an extremely large index contrast of $\Delta\mathrm{Re}(n) \sim -3.4$ was achievable simply by applying a gate voltage, and the observed value was unprecedented and hardly found in nature and can be increased further by using more advanced gating techniques. Second, we have provided compelling evidence that supports the possibility of achieving ultrafast optical control of the refractive index at a picosecond time scale. Spectrally- and temporally-resolved THz dynamics show that the strong coupling between the optically-excited graphene and the resonance of the metamaterial led to optically-controlled capacitive coupling in the graphene metamaterial, manifested by an increase of the on-resonance transmission. Third, we have presented a detailed investigation of the gate-dependent ultrafast Dirac fermion relaxation dynamics. By electrically changing the Fermi-level, we can understand that optical phonon scattering and acoustic phonon scattering are the key limiting factors in achieving ultra-high-speed index modulation. However, we emphasize that the relaxation process was significantly faster than that of almost any other semiconductor devices. Thus, graphene, if used as an active layer, may have a great advantage in the ultrafast operation of various THz devices, as well as in the index modulation of THz metamaterials for tunable transformation optics.

Methods

Fabrication of the graphene metamaterial. All metallic parts of the refractive index tunable metamaterial were made of 100-nm-thick gold with a 10-nm-thick chromium adhesion layer. The construction of the grapheme metamaterial was initiated by the spin-coating of a polyimide solution (PI-2610, HD MicroSystems) onto a sacrificial silicon wafer. After a two-step baking process, the polyimide film was fully cured, resulting in a final thickness of 1 μm. To define the transparent wire electrode, UV photolithography and electron-beam evaporation were followed by a metal lift-off technique. The metallic meta-atoms were patterned by repeating the same polyimide stacking processes and metal patterning as employed for the first layer. Then, commercially-available graphene from Graphene Square, Inc., grown by CVD onto copper film, was transferred to the entire area of the metamaterial (10×10 mm^2). After the graphene transfer, a ground electrode was defined on the graphene layer using a shadow mask, and we finally covered the device with a 1-μm-thick polyimide film. After opening the electrical contact via oxygen plasma etching of the covered polyimide film, the thin, substrate-free, flexible tunable graphene metamaterials were peeled off of the silicon substrate, as shown in Fig. 1b. Finally, the active graphene metamaterial was soldered to a drilled PCB substrate.

Optical-pump THz-probe spectroscopy. To characterize the electrical and optical modulation of the refractive index of the fabricated graphene metamaterial, we conducted optical-pump THz-probe spectroscopy together with electrical gating. The graphene metamaterial was excited by a nearly bandwidth-limited ultrashort 50 fs pulse with a photon energy of 1.55 eV delivered from a 250-kHz Ti:sapphire regenerative amplifier (Coherent RegA 9050). A fraction of the amplifier output was used to generate the THz pulse via optical rectification in a 500-μm-thick <110>

ZnTe nonlinear crystal. The collimated THz field was focused with a two-inch gold-coated off-axis parabolic mirror onto the high index graphene metamaterial. To detect the transmitted THz field through the sample, we used field-resolved electro-optic sampling in the same ZnTe crystal. The measured transient THz response directly reflected the dynamics of the complex $\Delta\varepsilon(\omega)$ or $\Delta\sigma(\omega)$, and the two are related by $\Delta\varepsilon(\omega) = \Delta\varepsilon_1(\omega) + i\Delta\varepsilon_2(\omega) = -\Delta\sigma_2(\omega)/\omega\varepsilon_0 + i\Delta\sigma_1(\omega)/\omega\varepsilon_0$. All measurements were performed at room temperature.

1. Haw, M. Holographic data storage: The light fantastic. *Nature* **422**, 556–558 (2003).
2. Ashkin, A. *et al.* Optically-induced refractive index inhomogeneities in $LiNbO_3$ and $LiTaO_3$. *Appl Phys Lett* **9**, 72–74 (1966).
3. Kirby, K. W. & DeShazer, L. G. Refractive indices of 14 nonlinear crystals isomorphic to KH2PO4. *J. Opt. Soc. Am. B* **4**, 1072–1078 (1987).
4. Würthner, F. *et al.* ATOP Dyes. Optimization of a Multifunctional Merocyanine Chromophore for High Refractive Index Modulation in Photorefractive Materials. *Journal of the American Chemical Society* **123**, 2810–2824 (2001).
5. Pendry, J. B., Holden, A. J., Robbins, D. J. & Stewart, W. J. Magnetism from conductors and enhanced nonlinear phenomena. *IEEE Transactions on Microwave Theory and Techniques* **47**, 2075–2084 (1999).
6. Smith, D. R., Padilla, W. J., Vier, D. C., Nemat-Nasser, S. C. & Schultz, S. Composite medium with simultaneously negative permeability and permittivity. *Phys Rev Lett* **84**, 4184–4187 (2000).
7. Choi, M. *et al.* A terahertz metamaterial with unnaturally high refractive index. *Nature* **470**, 369–373 (2011).
8. Yoon, H., Yeung, K. Y. M., Umansky, V. & Ham, D. A Newtonian approach to extraordinarily strong negative refraction. *Nature* **488**, 65–69 (2012).
9. Chen, H. T. *et al.* Active terahertz metamaterial devices. *Nature* **444**, 597–600 (2006).
10. Driscoll, T. *et al.* Memory Metamaterials. *Science* **325**, 1518–1521 (2009).
11. Xiao, S. *et al.* Loss-free and active optical negative-index metamaterials. *Nature* **466**, 735–738 (2010).
12. Liu, M. *et al.* Terahertz-field-induced insulator-to-metal transition in vanadium dioxide metamaterial. *Nature* **487**, 345–348 (2012).
13. Nikolaenko, A. E. *et al.* THz bandwidth optical switching with carbon nanotube metamaterial. *Opt. Express* **20**, 6068–6079 (2012).
14. Zhang, S. *et al.* Photoinduced handedness switching in terahertz chiral metamolecules. *Nat Commun* **3**, 942 (2012).
15. Lee, S. H. *et al.* Switching terahertz waves with gate-controlled active graphene metamaterials. *Nat Mater* **11**, 936–941 (2012).
16. Geim, A. K. & Novoselov, K. S. The rise of graphene. *Nat Mater* **6**, 183–191 (2007).
17. Nair, R. R. *et al.* Fine Structure Constant Defines Visual Transparency of Graphene. *Science* **320**, 1308 (2008).
18. Wang, F. *et al.* Gate-variable optical transitions in graphene. *Science* **320**, 206–209 (2008).
19. Sensale-Rodriguez, B. *et al.* Broadband graphene terahertz modulators enabled by intraband transitions. *Nat Commun* **3**, 780 (2012).
20. Ju, L. *et al.* Graphene plasmonics for tunable terahertz metamaterials. *Nat Nanotechnol* **6**, 630–634 (2011).
21. Weis, P. *et al.* Spectrally Wide-Band Terahertz Wave Modulator Based on Optically Tuned Graphene. *Acs Nano* (2012).
22. Echtermeyer, T. J. *et al.* Strong plasmonic enhancement of photovoltage in graphene. *Nat Commun* **2**, 458 (2011).
23. Sun, D. *et al.* Ultrafast Relaxation of Excited Dirac Fermions in Epitaxial Graphene Using Optical Differential Transmission Spectroscopy. *Phys Rev Lett* **101**, 157402 (2008).
24. George, P. A. *et al.* Ultrafast Optical-Pump Terahertz-Probe Spectroscopy of the Carrier Relaxation and Recombination Dynamics in Epitaxial Graphene. *Nano Lett* **8**, 4248–4251 (2008).
25. Dawlaty, J. M., Shivaraman, S., Chandrashekhar, M., Rana, F. & Spencer, M. G. Measurement of ultrafast carrier dynamics in epitaxial graphene. *Appl Phys Lett* **92**, 042116–042113 (2008).
26. Tse, W.-K. & Das Sarma, S. Energy relaxation of hot Dirac fermions in graphene. *Phys Rev B* **79**, 235406 (2009).
27. Sun, B. Y., Zhou, Y. & Wu, M. W. Dynamics of photoexcited carriers in graphene. *Phys Rev B* **85**, 125413 (2012).
28. Adam, S., Hwang, E. H., Galitski, V. M. & Das Sarma, S. A self-consistent theory for graphene transport. *Proceedings of the National Academy of Sciences* **104**, 18392–18397 (2007).
29. Smith, N. V. Classical generalization of the Drude formula for the optical conductivity. *Phys Rev B* **64**, 155106 (2001).
30. Breusing, M. *et al.* Ultrafast nonequilibrium carrier dynamics in a single graphene layer. *Phys Rev B* **83**, 153410 (2011).
31. Kaasbjerg, K., Thygesen, K. S. & Jacobsen, K. W. Unraveling the acoustic electron-phonon interaction in graphene. *Phys Rev B* **85**, 165440 (2012).

Acknowledgments

The work at KAIST (S.H.L., H.-D.K. and B.M.) was supported by the National Research Foundation of Korea (NRF) grant funded by the Korea government (MEST) (No. 2012-0001981, 2012-0006653, 2012-0008746, 2012-0000545, and 2012-054188) and the World Class Institute (WCI) Program of the National Research Foundation of Korea (NRF) funded by the Ministry of Education, Science and Technology of Korea (MEST). (NRF Grant Number: WCI 2011-001). The work at Yonsei (J. C. and H. C.) was supported by Basic Research Program through the National Research Foundation of Korea (NRF) funded by the Ministry of Education, Science and Technology (No. 2011-0013255), the NRF grant funded by the Korean government (MEST) (NRF-2011-220-D00052, No.2011-0028594, No.2011-0032019) and the LG Display academic industrial cooperation program.

Author contributions

H.C. and B.M. conceived the original idea. S.H.L. and H.-D.K. fabricated the samples and measured electrical modulation properties. J.C. performed optical pump-terahertz probe measurement. All of the authors analysed the data and wrote the manuscript.

Additional information

Supplementary information accompanies this paper at http://www.nature.com/scientificreports

Competing financial interests: The authors declare no competing financial interests.

How to cite this article: Lee, S.H., Choi, J., Kim, H.-D., Choi, H. & Min, B. Ultrafast refractive index control of a terahertz graphene metamaterial. *Sci. Rep.* **3**, 2135; DOI:10.1038/srep02135 (2013).